J-Integral Estimates for Strain-Hardening Materials in Ductile Fracture Problems

Satya N. Atluri* and Michihiko Nakagaki†
Georgia Institute of Technology, Atlanta, Ga.

A finite-element procedure is developed to analyze plane ductile fracture problems in the presence of large-scale yielding near the crack tip. Strain and stress singularities near the crack tip, corresponding to the strain-hardening material model, are embedded in elements near the crack tip. The developed elastic-plastic incremental finite-element method is based on a hybrid displacement model. The results for the J-integral at various load levels, for several standard fracture-toughness test specimens, are compared with available experimental results. The implication of the results in predicting initiation of crack growth, and its stability, in ductile materials is discussed.

Introduction

THE structure of the dominant singularity in stresses and strains near a crack tip in plane problems, for power-law hardening materials, has been studied by Hutchinson[1] and Rice and Rosengren.[2] Within the limitations of a small-strain J_2 deformation theory of plasticity, the amplitude of the foregoing dominant singularity, for pure mode problems, is related directly to the well-known J integral introduced by Rice[3] and earlier by Eshelby.[4] Thus the J integral can be taken to be a convenient measure of the strength of singularity in such problems.

The J integral is defined by

$$J=\int_\Gamma \left(w\mathrm{d}y - T_K \frac{\partial u_K}{\partial x}\,\mathrm{d}s\right) \tag{1}$$

where x, y are coordinates normal to the crack front, y being perpendicular to the crack surface; $\mathrm{d}s$ is a differential arc length along any contour Γ, beginning along the bottom surface of the crack and ending along the top surface; W is the strain energy density; T_K are components of traction on the surface of the interior body cut by Γ; and u_K are displacement components. The J integral is path-independent if the strain energy is a single-valued function of the strains. This is the case if the material is nonlinearly elastic, or in the case of an elastic-plastic material if a J_2 deformation theory is used, so long as the effective stress is not decreased. In the case of an elastic solid (linear or nonlinear), the J integral can be interpreted as the energy flow toward the crack tip per unit of crack extension. This energy release interpretation of J cannot be applied to the process of crack extension in elastic-plastic solids, even with a J_2 deformation theory. However, using a J_2 deformation theory, the J integral can be interpreted as the potential energy difference between two identically loaded bodies having neighboring crack sizes, i.e., $\partial P/\partial \ell$, where P is the potential energy and ℓ is the crack length.

Under a J_2 flow theory of plasticity, the physical significance of J as a measure of the characteristic crack-tip elastic-plastic stress/strain field still is valid. When a J_2 flow theory is used, the path independence of the J integral, even under monotonic loading, cannot be established. However, under monotonic loading, the use of a total strain theory is justifiable in studies of stress/strain fields near a stationary crack because approximately proportional loading occurs. During the loading of a cracked body from the virgin state to the critical state, the effective stress can be expected to increase everywhere in the region. Thus, under monotonic loadings, approximate path independence of the J integral may be expected even under J_2 flow theory of plasticity. Thus, the J integral, defined by

$$J=\int_\Gamma \left\{\left(\int_0^{\epsilon'_{ij}} \sigma_{ij}\mathrm{d}\epsilon'_{ij}\right)\mathrm{d}y - T_K \frac{\partial u_K}{\partial x}\,\mathrm{d}s\right\} \tag{2}$$

where σ_{ij} is the stress at any point and $\mathrm{d}\epsilon'_{ij}$ is the *total* incremental strain at the point, may be taken as a variable specifying the severity of the conditions at the crack tip when large-scale yielding is present.

If the magnitudes of the loads are designated by a generalized load parameter Q, then $J=J(Q)$. The critical generalized load Q_C at which crack growth initiation occurs in plane, ductile, fracture problems can be stated by the condition $J=J_C=J(Q_C)$. It is noted at this point that this criterion ($J=J_C$) is a criterion for initiation of crack growth only, without any statement of stability or instability of such crack growth.

In recent experiments, Begley and Landes[5] have demonstrated the potential of the J integral as a fracture initiation criterion in the large-scale yielding range. In experimentally determining critical J in elastic-plastic problems, Begley and Landes[5] utilized the interpretation of J as the rate of change with respect to the crack length of the area under the load vs the load-point displacement curves of standard fracture test specimens such as the three-point bend specimen and the compact tension specimen. Thus the original experimental protocol of Begley and Landes calls for testing virgin specimens with different crack sizes. For fracture test specimens such as the aforementioned, where the only geometric dimension of interest is the uncracked ligament length, recently Rice et al.[6] have shown that the J integral can be evaluated from a single, experimentally generated, load-displacement record.

Turning to analytical estimation procedures, when small-scale yielding exists near the crack tip, J is simply related to the elastic stress-intensity factor. For large-scale yielding, such simple calculations are not possible, since J depends on the geometry, applied loadings, and material properties in a complicated way. In the analysis of fracture test specimens, a simple approximate procedure for estimation of J has been used by Bucci et al.[7] who "extrapolate" from small-scale yielding range to fully plastic range using Irwin's "plasticity

Presented at the AIAA/ASME/SAE 17th Structures, Structural Dynamics, and Materials Conference, King of Prussia, Pa., May 5-7, 1976 (in bound volume of Conference papers, no paper number); submitted May 27, 1976; revision received Feb. 33, 1977.

Index categories: Structural Statics; Materials, Properties of.

*Professor, School of Engineering Science and Mechanics. Member AIAA.

†Postdoctoral Fellow, School of Engineering Science and Mechanics.

corrections." On the other hand, for pure power-law hardening materials ($\epsilon \sim \sigma^n$), using a deformation theory of plasticity, simple, approximate procedures for estimating J were presented recently by Goldman and Hutchinson.[8] In Ref. 8, a circular core element with embedded dominant singularity of the type derived in Refs. 1 and 2 is used near the crack tip. The θ dependence of this dominant singular term (where r and θ are polar coordinates centered at the crack tip) is determined in Refs. 1 and 2 from the numerical solution for a nonlinear, fourth-order, ordinary differential equation for each value of the exponent n in the material power-hardening law ($\epsilon \sim \sigma^n$). For mixed-mode problems, the determination of this θ dependence is much more complicated.[9] Moreover, the use of J_2 deformation theory of plasticity in Ref. 8 makes it invalid in situations where significant unloading is observed. Such unloading situations are observed in cases involving stable crack growth.

In view of the preceding discussion, the research presently reported has the objective of developing a numerical procedure to estimate J in arbitrary plane problems of ductile fracture with arbitrary geometry, some of the details of which are as follows:

1) Circular-sector-shaped embedded singularity elements are developed near the crack tip. The correct r dependence of the dominant singular solution, corresponding to the nonlinear material model, was embedded in these near-tip elements, whereas the θ variation was approximated in each sector element in the sense of the finite-element method.

2) Continuity of displacements and tractions is maintained between near-tip elements with singular stress/strain assumptions and the far-field elements with regular stress/strain assumptions, through a hybrid displacement finite-element model, as was done in linear elastic fracture problems.[10,11]

3) A J_2 flow theory of plasticity and arbitrary kinematic hardening is used which will model the Bauschinger effect accurately under fully reversed and cyclic loading.

4) An incremental finite-element solution procedure is used which will be suitable in the limiting case of elastic-perfectly-plastic materials, as well as cyclic loading situations: the "initial stress iteration" approach as originally proposed.

5) A more accurate method is used for plasticity iterations in each increment. The more common approach in the literature is to use "constant-stress' elements, and, based on the stress level in the element, the whole element either yields or stays elastic. Thus, in problems such as the present, where the yield zones near the crack tip play a dominant role in the analysis and its interpretation, in order to obtain a reasonably accurate description of the yield zone, a very fine finite-element mesh is needed. However, if higher-order elements are used, and if "plasticity-correction" iterations are performed at several points within the element, it then becomes possible to give a smoother definition of the yield zone. Thus, a portion of the element in the present formulation can yield, whereas the rest of the element can remain elastic. The present analysis also is based on a small-deformation, small-strain theory.

In the following, we present detailed results and their comparison with available experimental data, for the case of a compact tension specimen made of A533B pressure vessel steel. A discussion of the implication of these results in predicting crack growth initiation and its stability in ductile materials is presented.

Theoretical Formulation

Hybrid Displacement Finite-Element Model for Incremental Elastic-Plastic Solution

The applicability of a hybrid-displacement type of finite-element model to enforce continuity of displacements and equilibrium of tractions between near-tip elements (with singular stress/strains) and far-field elements (with regular polynomial-type stresses/strains) has been discussed in detail[10,11] in the context of problems of linear elastic fracture mechanics. The same basic theory has been extended here to formulate an incremental procedure for elastic-plastic analysis of cracked structures.

The analysis procedure is based on a small-strain, small-displacement, incremental flow theory of plasticity. In general, we define S_N to be the state of the body before the addition of the Nth load increment, whereas S_{N+1} is the state after the Nth load increment. In S_N, the states of stress, strain, and deformation in the elastic-plastic cracked body are presumed to be known. During the process of the Nth increment, this state is considered to be in a state of "initial stress." In the following, we treat, as a generic case, the transition of the cracked body from a reference S_N to S_{N+1}, during which the incremental stresses will be calculated first from the linear elastic constitutive law. If there is plastic flow in the body, this elastic estimate of incremental stresses will be higher than in the actual strain-hardening body. The actual stress and strain increments in the presence of plasticity then will be obtained by modifying the elastic predictions using the "initial-stress iteration" approach in each increment, as originally proposed by Zienckiewicz et al.[12]

Analogous to the variational principle governing the hybrid-displacement model for linear problems,[10,11] the incremental variational principle governing the present formulation can be stated as $\delta\Delta\pi = 0$ where

$$\Delta\pi(\Delta u_i, \Delta v_i, T_{Li}) = \sum_{m=1}^{M} \left\{ \int_{V_m} \left(\left[\sigma_{ij}^0 - \Delta\sigma_{ij}^* + \tfrac{1}{2}\Delta\epsilon_{k\ell}^t E_{ijk\ell} \right] \cdot \Delta\epsilon_{ij}^t - \left[F_i^0 + \Delta F_i \right] \Delta u_i \right) dV + \int_{\partial V_m} T_{Li}(\Delta v_i - \Delta u_i)\, ds - \int_{S_{\sigma_m}} (\bar{T}_i^0 + \Delta\bar{T}_i)\Delta v_i\, ds \right\} \quad (3)$$

where

V_m = domain of the mth finite element

∂V_m = entire boundary of the mth element

$S_{\sigma m}$ = a portion of ∂V_m where surface tractions are given

$\sigma_{ij}^0, F_i^0, \bar{T}_i^0$ = initial stress, body force, and surface traction, respectively, in the state S_N

$\Delta\sigma_{ij}^*$ = adjustment to the elastic overprediction of stress in each "plasticity-correction" iteration during the current increment ("initial-stress" iteration of Zienckiewicz et al.[12])

Δu_i = arbitrarily assumed displacements, in each element, which need not satisfy interelement compatibility a priori; in elements surrounding the crack tip, displacements corresponding to the Hutchinson-Rice-Rosengren singularities, for hardening materials, are included

$\Delta\epsilon_{ij}^t$ = $\frac{1}{2}(\Delta u_{i,j} + \Delta u_{j,i})$ = incremental total strain

Δv_i = independently assumed displacements, at ∂V_m, which inherently satisfy interelement compatibility criteria

T_{Li} = Lagrange multiplier to enforce the compatibility condition $\Delta u_i = \Delta v_i$ at ∂V_m

$E_{ijk\ell}$ = linear elasticity tensor for the material

$\Delta\sigma_{ij}$ = true stress increment in the current increment in the presence of plasticity

$\Delta\sigma_{ij} = E_{ijk\ell}\Delta\epsilon_{k\ell}^t - \Delta\sigma_{ij}^* \equiv E_{ijk\ell}^t \Delta\epsilon_{k\ell}^t$

$E_{ijk\ell}^t$ = current constitutive relation tensor, relating total increment of stress to total increment of strain

$\Delta F_i, \Delta\bar{T}_i$ = prescribed increments of body forces and surface tractions, respectively, in the current increment

The matrix $E^t_{ijk\ell}$ is derived from the classical plasticity theory based on 1) Huber-Mises-Hencky yield condition, 2) Drucker's normality condition for incremental plastic strain, and 3) Ziegler's modification of Prager's kinematic hardening rule. The form of $E^t_{ijk\ell}$ for the case of plane strain and plane stress, respectively, is given in the Appendix.

The Euler equations corresponding to $\delta\Delta\pi(\delta\Delta u_i;\ \delta T_{Li};\ \delta\Delta v_i) = 0$ lead to

$$(E_{ijk\ell}\Delta\epsilon^t_{k\ell} - \Delta\sigma^*_{ij})_{,j} + \Delta F_i + [\sigma^0_{ij,j} + F^0_i] = 0 \text{ in } V_m \tag{4}$$

$$(\sigma^0_{ij} + E_{ijk\ell}\Delta\epsilon^t_{k\ell} - \Delta\sigma^*_{ij})\nu_j = T_{Li} \text{ at } \partial V_m \tag{5}$$

$$\Delta u_i = \Delta$$

$$\Delta u_i = \Delta v_i \text{ at } \partial V_m \tag{6}$$

$$T_{Li} = T^0_i + \Delta\bar{T}_i \text{ at } S_{\sigma_m} \tag{7}$$

Equation (4) refers to the equilibrium of total stresses in S_{N+1}. If state S_N were in true equilibrium, the term $\sigma^0_{ij,j} + F^0_i$ in Eq. (4) would be equal to zero. However, because of the inherent numerical errors in the piecewise linear incremental solution process, the state S_N may not be in true equilibrium. Thus, retaining the prior-equilibrium error term $\sigma^0_{ij} + F^0_i = \epsilon_i \neq 0$ in Eq. (4) leads to an equilibrium check iteration, similar to the one used by Hofmeister et al.[13]

Equation (5) states that the tractions derived from the assumed incremental interior displacements match independently assumed boundary tractions (T_{Li}). Finally, Eq. (6) is the statement of interelement displacement compatibility which is enforced, in the present method, by means of Lagrange multipliers T_{Li}.

One makes the finite-element approximations

$$\{\Delta u\} = [A]\ \{\beta\};\ \{\Delta v\} = [L]\ \{\Delta q\};\ \{T_{Li}\} = [R]\ \{\alpha\} \tag{8}$$

where β and α are undetermined parameters, and Δq are incremental nodal displacements. The functions in the matrices A and R are chosen appropriately to correspond to singular stresses/strains in elements in the immediate vicinity of the crack tip but are otherwise arbitrary. The functions in the matrix L are functions at the boundary ∂V_m which uniquely interpolate for Δv at ∂V_m in terms of relevant nodal Δq.

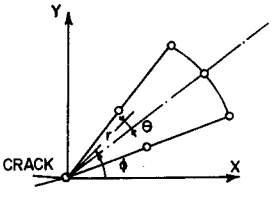

Fig. 1 Nomenclature for a "singular" element.

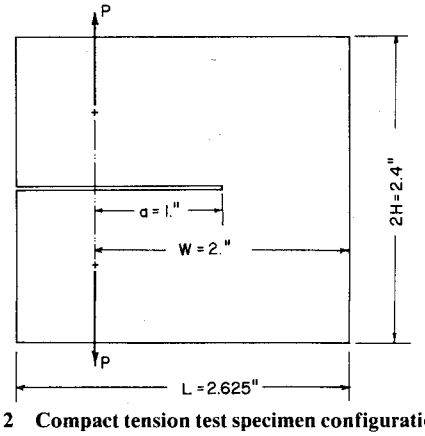

Fig. 2 Compact tension test specimen configuration.

The element total strains are derived from the element $\{\Delta u\}$, as $\{\Delta\epsilon^t\} = [W]\ \{\beta\}$. Using the approximations (8) in the functional of Eq. (3), we see that

$$\Delta\pi(\alpha,\beta,q) = \sum_{m=1}^{M}\left(\frac{1}{2}[\beta]\ [H]\ \{\beta\} - [\beta]\ \{S' - S^0\}\right.$$

$$\left. + [\Delta q][G]\{\alpha\} - [\beta][P_I]\{\alpha\} - [\Delta q]\{\Delta F_I\} - [\Delta q]\{\Delta F_0\}\right) \tag{9}$$

where

$$[H] = \int_{V_m}[W]^T[E][W]\mathrm{d}V;\quad \{S'\} = \int_{V_m}[W]^T\{\Delta\sigma^*\}\mathrm{d}V$$

$$\{S^0\} = \int_{V_m}[W]^T\{\sigma^0\}\mathrm{d}V;\quad [G] = \int_{\partial V_m}[L]^T[R]\mathrm{d}s$$

$$[P_I] = \int_{\partial V_m}[A]^T[R]\mathrm{d}s;\quad \{\Delta F_I\} = \int_{S_{\sigma_m}}[L]^T\{\Delta\bar{T}\}\mathrm{d}s$$

and that

$$\{\Delta F^0\} = \int_{S_{\sigma_m}}[L]^T\{\bar{T}^0\}\mathrm{d}s \tag{10}$$

where $[E]$ is the matrix of elasticity constants, and $\{\sigma^0\}$ and $\{\Delta\sigma^*\}$ are representations for σ^0_{ij} and $\Delta\sigma^*_{ij}$, respectively.

Since the undetermined parameters $\{\alpha\}$ and $\{\beta\}$ are arbitrary and independent for each element, taking variations of $\Delta\pi$ with respect to $\{\beta\}$ and $\{\alpha\}$ yields, respectively, for each element

$$[H]\{\beta\} - \{S'\} - \{S^0\} - [P_I]\{\alpha\} = 0 \tag{11}$$

$$[G]^T\{\Delta q\} - [P_I]^T\{\beta\} = 0 \tag{12}$$

Using the preceding equations to express $\{\alpha\}$ and $\{\beta\}$, for each element, in terms of the respective $\{\Delta q\}$ of each element, the functional $\Delta\pi$ can be expressed entirely in terms of the element nodal displacement $\{\Delta q\}$ only. Thus,

$$\Delta\pi(\Delta q) = \sum_{m=1}^{M}\left(\frac{1}{2}[\Delta q][K_m]\{\Delta q\}\right.$$

$$\left. - [\Delta q]\{\Delta F_I + \Delta Q^0 + \Delta Q'\} + \text{const}\right) \tag{13}$$

where

$$[K_m] = [G][P_I]^{-1}[H][P_I]^{-T}[G]^T \tag{14a}$$

$$\{\Delta Q^0\} = -[G][P_I]^{-1}\{S^0\} + \{\Delta F^0\} \tag{14b}$$

and

$$\{\Delta Q'\} = [G][P_I]^{-1}\{S'\} \tag{15}$$

Using the common procedure for "assembling" the finite elements, the functional $\Delta\pi$ is expressed in terms of the nodal displacements of the entire structure, Δq^*. Thus,

$$\Delta\pi = \tfrac{1}{2}[\Delta q^*][K]\{\Delta q^*\} - [\Delta q^*]\{\Delta F_I + \Delta Q^0 + \Delta Q'\} \tag{16}$$

From Eq. (16), the final finite-element equations can be derived as

$$[K]\{\Delta q^*\} = \{\Delta F_I\} + \{\Delta Q^0\} + \{\Delta Q'\} \tag{17}$$

where $[K]$ is the linear-elastic stiffness matrix of the entire structure, $\{\Delta q^*\}$ are the nodal displacements of the system, $\{\Delta F_I\}$ are the consistent nodal forces in the current increment, $\{\Delta Q^0\}$ is the "nodal-force-imbalance" vector to check the equilibrium of the structure at the beginning of the increment, and $\{\Delta Q'\}$ are the equivalent nodal forces due to

the iterative "plasticity-correction" adjustments associated with the "initial-stress-iteration" approach. Thus, in the present solution procedure, during each increment $\{\Delta Q'\}$ are taken to be zero initially, and at the end of the plasticity correction iteration they should converge to zero.

Field Assumptions for a Circular-Sector-Shaped "Singular Element" Near the Crack Tip

The preceding formulation calls for assumed functions, in each element, for 1) element interior-displacement field Δu_i; 2) element boundary-displacement field Δv_i, and 3) an equilibrated element boundary-traction field T_{Li}. Such assumptions for elements away from the crack tip already have been presented.[11] Only the assumption for circular-sector-shaped "singular elements" (with six nodes, as shown in Fig. 1) surrounding the crack tip is given here. It is noted first that the structure of the dominant singularity, for pure-mode plane problems and for the nonlinear material model employed, was shown in Refs. 1 and 2 to be

$$\sigma_{ij} \sim K_p r^{-1/n+1} \tilde{\sigma}_{ij}(\theta); \quad \epsilon_{ij} \sim K_\epsilon r^{-n/n+1} \tilde{\epsilon}_{ij}(\theta)$$

and

$$u_i \sim K_\epsilon r^{1/n+1} \tilde{u}_i(\theta) \tag{18}$$

where (r,θ) are polar coordinates centered at the crack tip, and n is the exponent in the material-hardening law. With Eq. (18) in mind, the "singular element," the following assumptions have been made.

Element Interior Displacement (Singular Element)

$$\begin{aligned}\Delta u_r = {} & \beta_1 r + 2\beta_2 r\theta + \beta_3 r\theta^2 + \beta_5 r^2 + \beta_6 r^2\theta \\ & + \beta_{10}\cos\varphi r^{1/n+1} + \beta_{11}\cos\varphi r^{1/n+1}\theta \\ & + \beta_{12}\cos\varphi r^{1/n+1}\theta^2 + \beta_{13}\sin\varphi r^{1/n+1} \\ & + \beta_{14}\sin\varphi r^{1/n+1}\theta + \beta_{15}\sin\varphi r^{1/n+1}\theta^2\end{aligned} \tag{19}$$

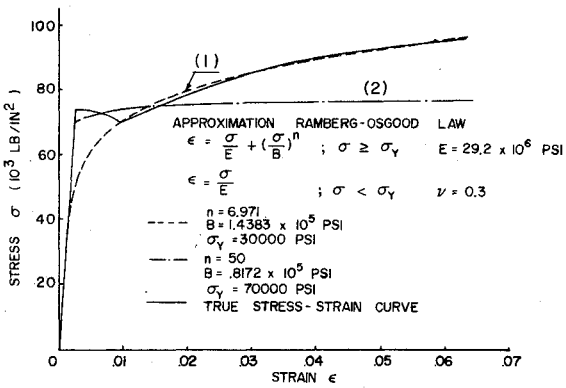

Fig. 3 Uniaxial stress-strain curve for A533B steel.

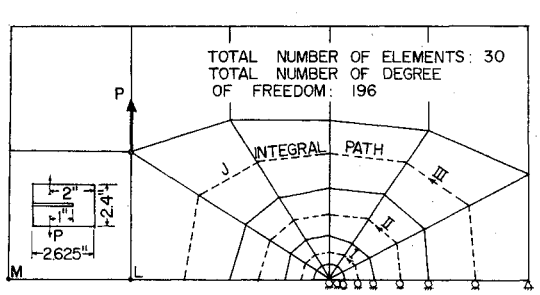

Fig. 4 Finite-element model for the compact tension specimen.

$$\begin{aligned}\Delta u_\theta = {} & \beta_2 r + \beta_4 r\theta + \beta_7 r\theta^2 + \beta_8 r^2 + \beta_9 r^2\theta \\ & - \beta_{10}\sin\varphi r^{1/n+1} - \beta_{11}\sin\varphi r^{1/n+1}\theta \\ & - \beta_{12}\sin\varphi r^{1/n+1}\theta^2 + \beta_{13}\cos\varphi r^{1/n+1} \\ & + \beta_{14}\cos\varphi r^{1/n+1}\theta + \beta_{15}\cos\varphi r^{1/n+1}\theta^2\end{aligned} \tag{20}$$

where φ is the global angular coordinate, and θ is the angle measured from the element's symmetric axis. It has been established that the combination of a regular displacement field (β_1 through β_9) and the asymptotic displacement field (β_{10} through β_{15}) allows one to use "singular elements," near the crack tip, of as large a size as a tenth of the crack length without loosing numerical accuracy.

Element Boundary-Displacement Field (Singular Element)

For the "singular element," Δv_i is assumed to be 1) along AB, AC of the type $a_1 r^{1/n+1} + a_2 r + a_3$, and 2) along BC of the type $b_1 + b_2\theta + b_3\theta^2$. The preceding assumption can be seen to satisfy the interelement displacement compatibility.

Element Boundary-Traction Field (Singular Element)

The tractions T_{Li} for the "singular element" are assumed from the stresses derived from the Airy stress function:

$$\begin{aligned}\psi(r,\theta) = {} & \alpha_1 r^2 + \alpha_2 r^2\theta + \alpha_3 r^2\theta^2 + \alpha_4 r^2\theta^3 + \alpha_5 r^3 \\ & + \alpha_6 r^3\theta + \alpha_7 r^3\theta^2 + \alpha_8 r^3\theta^3 + \alpha_9 r^4 + \alpha_{10} r^4\theta \\ & + \alpha_{11} r^4\theta^2 + \alpha_{12} r^4\theta^3 + \alpha_{13} r^{n+2/n+1} \\ & + \alpha_{14}\theta r^{n+2/n+1} + \alpha_{15}\theta^2 r^{n+2/n+1}\end{aligned} \tag{21}$$

Results

To evaluate the present numerical procedure, it has been applied to the case of a compact tension specimen, for which experimental results have been reported.[5] The specimen is of 1-in. thickness and of in-plane dimensions, as shown in Fig. 2, and is made of A533B pressure vessel steel, whose material property, i.e., uniaxial stress-strain curve, is shown in Fig. 3. This uniaxial stress-strain curve, for the convenience of numerical implementation, has been approximated closely by an appropriate Ramberg-Osgood law, as also shown in Fig. 3. Even though the loading of the compact tension specimen in the actual experiment involves a pin-hole in the specimen, the effect of this pin has not been simulated in the present numerical procedure; instead, a point loading has been assumed.

The experimental protocol in the original work of Begley and Landes[5] consisted in monotonically loading several virgin specimens, each with a different crack length. In specimens such as the compact tension, where the uncracked ligament is subject principally to bending but the load is applied by concentrated load P, it has been shown recently by Rice et al.[6] that the J integral can be evaluated directly from a single-specimen load-displacement curve; thus,

$$J = \frac{2}{b}\int_0^{\delta \text{ crack}} P(\mathrm{d}\delta_{\text{crack}}) \tag{22}$$

where b is the length of the uncracked ligament. Thus J has the simple definition of twice the work of deformation divided by the uncracked ligament length. The empirical formula, Eq. (22), for the compact tension specimen considers only the effect of the bending moment of the applied load at the net section ligament. More recently, Merkle and Corten[14] derived an improved formula for the J integral for the compact tension specimen, based on single-specimen test data for the load-displacement curve, which takes into ac-

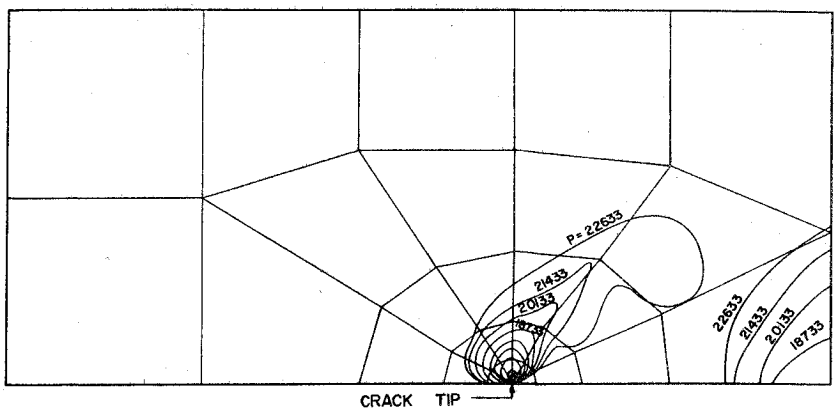

Fig. 5 Plastic yield zones at various load levels (plane strain, strain-hardening).

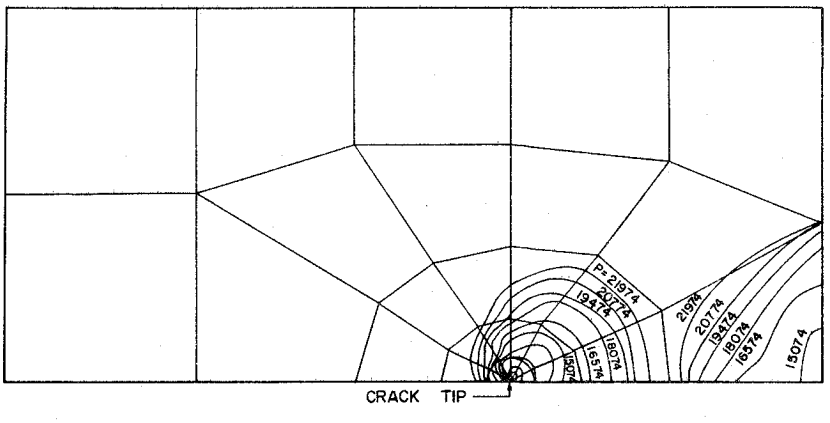

Fig. 6 Plastic yield zones at various load levels (plane stress, strain-hardening).

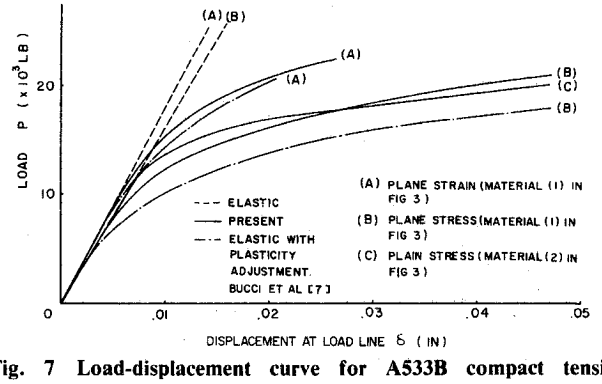

Fig. 7 Load-displacement curve for A533B compact tension specimen.

count the effects of both the axial force and bending moment at the net-section ligament. This empirical formula[14] can be stated as

$$J=\frac{1}{2}\frac{P^2}{B}\frac{\partial(1/K)}{\partial a}+\frac{2(1+\alpha)}{b(1+\alpha^2)}\int_0^{\Delta P}\left(\frac{P}{B}\right)d\Delta_P + \frac{2}{b}\alpha\frac{(1-2\alpha-\alpha^2)}{(1+\alpha^2)^2}\int_0^{P/B}\Delta_p d\left(\frac{P}{B}\right) \tag{23}$$

where

$$\alpha=\left[\left(\frac{a}{c}\right)^2+2\left(\frac{a}{c}\right)+2\right]^{1/2}-\left(\frac{a}{c}+1\right)$$

and, furthermore, a = crack length, c = half the net-ligament width (see Fig. 2), P = applied force, B = specimen thickness, K = elastic stiffness at the load point, Δ_p = plastic displacement of the applied load due to the crack, and $b=2c$.

In the present numerical formulation, since stress/strain data at each point and at each load level are calculated, the J integral is evaluated numerically using the formula of Eq. (2) directly. This direct evaluation of J as a path integral has been carried out in the present study, along different paths at each load level, as shown in Fig. 4. The average of these four different path integrals is taken to be the valid J at the particular load level. Using the numerically evaluated P vs δ curve, the J integral also is evaluated using the empirical formulas just cited.[6-14] The presently computed J integral values will be compared with the experimental results of Begley and Landes.[5]

Detailed Results for the Compact Tension Specimen

First we note that, if in the assumed field functions for the "singular element" as detailed earlier one sets $n=1$, then the assumptions correspond to an approximation for the asymptotic solutions in the linear elastic case. Thus, in the first increment of the present procedure, setting $n=1$, the linear elastic case can be computed. The value of the normalized stress intensity factor, in the linear elastic case, as calculated directly from the built-in asymptotic stress/displacement field in the present procedure, was found to be $K_I/P=6.602$. This is in excellent agreement with that reported by Bucci et al.[7] for similar geometry, which is $K_I/P=6.79$. The J integral, for this linear elastic case, also was computed directly around different paths, as shown in Fig. 4. The average value of J for these paths (with a $\pm 3\%$ variation between the paths) was found to be 0.1477×10^{-5} lb-in./in.^{2} per unit load for the plane strain case, which corresponds to a value $K_I/P=6.880$.

To understand the influence of the assumption of the plane stress or, alternatively, the plane strain state in the 1-in.-thick specimen shown in Fig. 2, both cases were treated in the present elastic-plastic analysis. Figure 4 shows the finite-element model of the compact tension specimen which is used, with 30 elements, 93 nodes, and 170 degrees of freedom. Figure 5 shows the plastic zones in the specimen at various load levels, when the conditions of plane strain are invoked.

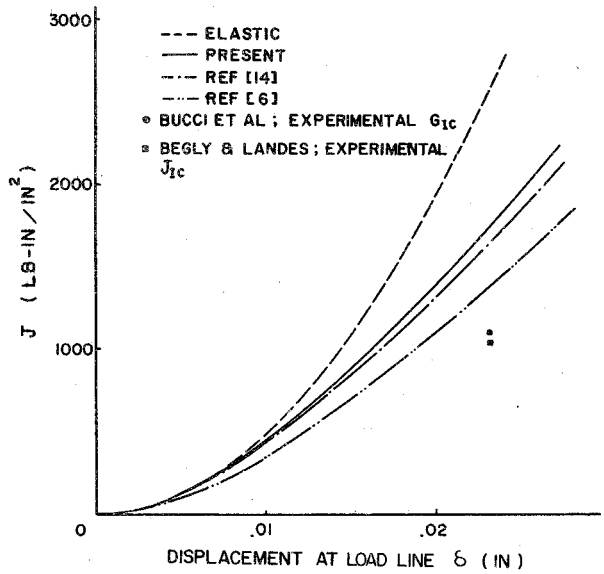

Fig. 8 J vs δ curves for compact tension specimen (plane strain condition).

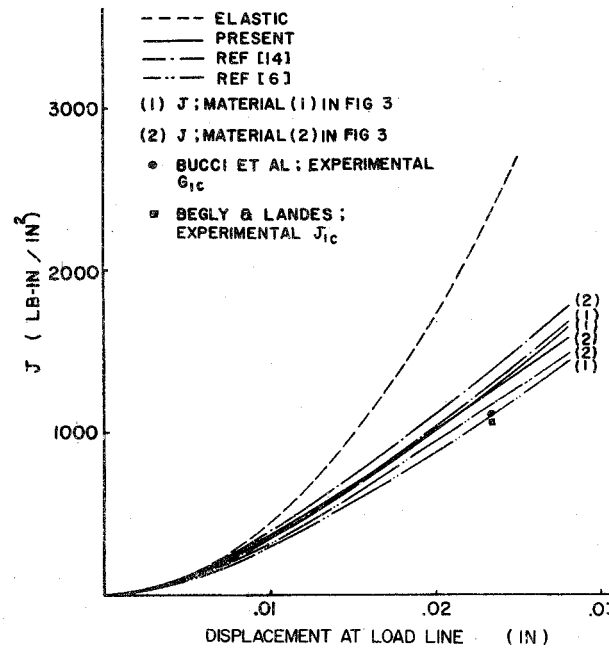

Fig. 9 J vs δ curves for compact tension specimen (plane stress condition).

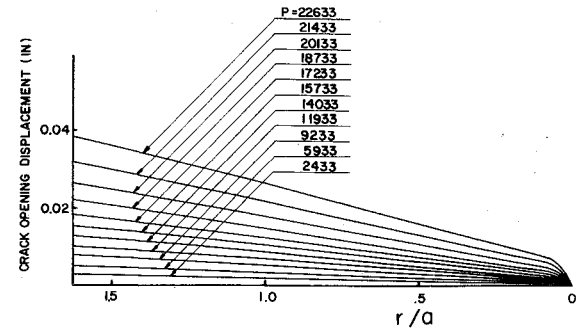

Fig. 10 Crack surface deformation profiles (plane strain, hardening).

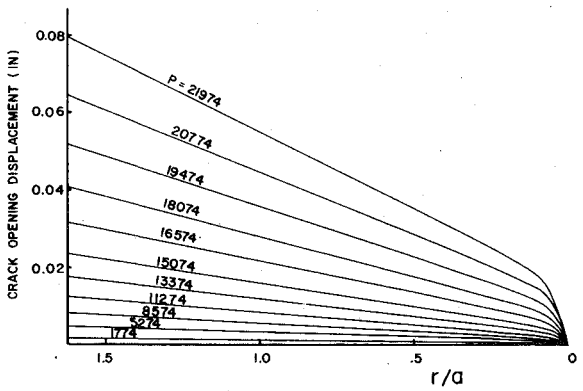

Fig. 11 Crack surface deformation profiles (plane stress, hardening).

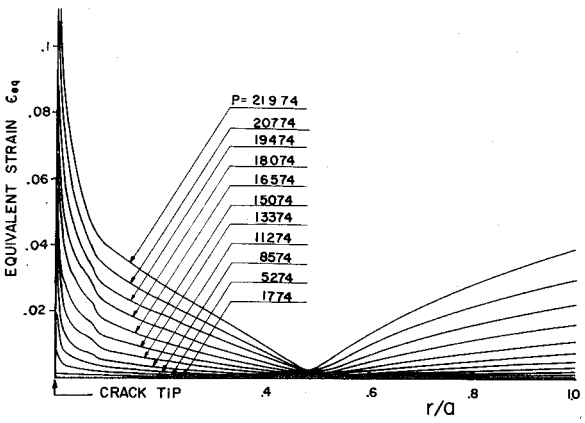

Fig. 12 Effective strain distribution in the uncracked ligament (plane stress, hardening).

Figure 6 likewise shows the yield zones in the specimen where plane stress conditions are assumed. It is interesting to note that, in the case of plane strain, the uncracked ligament immediately ahead of the crack tip does not yield even at a load of $P=22.5\ K_I/P$ whereas in the case of plane stress, at $P=20.8\ K_I/P$, almost the entire uncracked ligament has yielded. This uncontained plasticity in the case of plane stress is believed to have significant effects on slow, stable crack growth, in plane stress situations, which will be studied in a subsequent paper. Figure 7 shows the results for load-line displacement (at point L in Fig. 4) variation with load for the cases of plane stress and plane strain, obtained in the present analysis, using the Ramberg-Osgood material behavior approximation 1, as shown in Fig. 3. Also shown, for comparison, are the results for both plane strain and plane stress cases based on linear-elastic analysis, as well as the empirical results of Bucci et al.[7] based on elastic-perfectly-plastic material behavior assumption. It can be seen that, when the specimen yields, there is a substantial difference between the values of the load-point displacement (at the same load) for the cases of plane stress and plane strain. Moreover, in the plane strain case, there is a good agreement of the present results with those of Bucci et al.,[7] whereas such a comparison is rather poor in the case of plane stress.

Figure 8 shows the variation of the value of the J integral with the load-line displacement for the plane strain case. The J integral was calculated, using Eq. (2), over different paths, which are shown in Fig. 4. The average value of J for these paths (with a $\pm 3\%$ variation between the paths) is plotted in Fig. 8. Also shown for comparison purposes are estimates of J based on 1) linear-elastic theory (essentially a "small-scale yielding" approximation), 2) the computed load-displacement curve of Fig. 7 using the empirical formula of Ref. 6, and 3) computed load-displacement curve using the empirical formula of Ref. 14. The critical value of J_{Ic}, experimentally obtained by Begley and Landes for the present 1-in.-thick specimen, as well as G_{Ic} obtained by Bucci et al.[7] using a 12-in-thick specimen, also are shown. It can be seen from Fig. 8

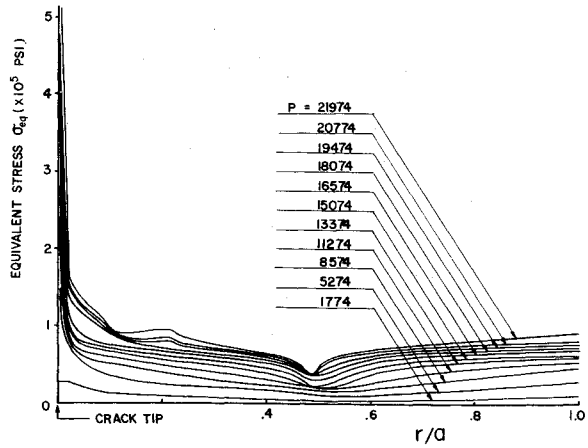

Fig. 13 Effective stress distribution in the uncracked ligament (plane stress, hardening).

that the present direct computation of J agrees well with the empirical formula of Merkle and Corten[14] rather than with that of Rice et al.[6] The substantial difference between the computed J_{Ic} (at $\delta_c \sim 0.023$ in.) and the experimental J_{Ic} obtained in Ref. 5 suggests that the plane strain assumption is very poor for the present 1-in.-thick specimen.

Figure 9 shows the variation of the average value of the directly computed J integral with the load-line displacement for the plane stress case. Once again, for comparison purposes, the estimation of J is shown, based on 1) linear-elastic theory, 2) the computed load-displacement curve using the empirical formula of Rice et al., and 3) the computed load-displacement curve using the relation given by Merkle and Corten. It can be seen that the empirical formula of Ref. 14 provides an excellent agreement with the present direct computation of J, whereas the formula of Rice et al. provides an underestimation by about 10%. The closeness of the present plane stress result for J (at $\delta \sim 0.023$ in.) and the experimental J of Begley and Landes[5] suggests that, for the present specimen of the 1-in. thickness, plane stress conditions prevail at the crack tip. The experimental result for J_{Ic} for the present specimen‡ obtained in Ref. 5 is still lower by about 14% than the present plane stress result. It is felt that this may be attributed to the possible presence of stable crack growth, in plane stress situations, prior to fracturing in specimens in the experiments. The numerical simulation of stable crack growth presently is being carried out by the authors and will be reported in a subsequent paper.

Figures 10 and 11 show the crack-surface deformation profiles, at various load levels, for the cases of plane strain and plane stress, respectively. In both cases, the blunting of the crack tip can be noticed at load levels greater than approximately 15 kips. To assess the effect of this blunting on the stress/strain states near the crack tip requires a finite deformation analysis, the results of which are reported elsewhere.[15] The distribution of the effective strain ahead of the crack tip, in the uncracked ligament, for the case of plane stress is shown in Fig. 12; Fig. 13 shows the distribution of the effective stress ahead of the crack tip in the uncracked ligament for the plane stress case.

Finally, to study the effects of the mathematical modeling of the uniaxial stress strain curve, an alternate Ramberg-Osgood law, closely approximating an elastic-perfectly-plastic behavior, was used. This curve was taken to be $\epsilon = \sigma/E + (\sigma/B_0)^n$ for $\sigma \geq \sigma_y$ and $\epsilon = \sigma/E$ for $\sigma < \sigma_y$ with $n = 50$, $B = 8.1 \times 10^4$ psi, $\sigma_y = 70 \times 10^3$ psi, and $E = 29.2 \times 10^6$ psi. Thus, this particular modeling corresponds almost to perfectly plastic behavior after $\sigma = 70 \times 10^3$ psi. No significant differences in the main result, namely, that for the J integral, were noticed, even though the results differed somewhat in detail for stresses, as compared with the Osgood approximation for the material behavior, as shown in Fig. 3. The differences between the results using the two different types of Ramberg-Osgood approximation to the stress-strain law can be seen in Figs. 7-9.

‡The experimentally determined crack-mouth opening (at point M in Fig. 4) of 0.07 in. corresponds to the crack-surface deformation at the load line (point L in Fig. 4) of about 0.023 in. as seen in Fig. 11.

Conclusions

From the preceding comparison of the results under both the plane stress and plane strain conditions and from the cited experimental results, it may be concluded that plane stress conditions prevail near the crack tip in the present 1-in.-thick compact tension specimen. It also has been established that, for compact tension test specimens, the empirical relation given by Merkle and Corten[14] is much more accurate than that given by Rice et al.[6] to evaluate J from single-specimen test data for the load vs displacement behavior.

The close agreement of the present J-integral results with the experimental data for the present compact tension specimen as well as other test specimens (not reported here because of space limitations) indicates that the present numerical procedure can be used to complete the J integral accurately in plane problems involving arbitrary domains, arbitrary loading that causes large-scale yielding near the crack, and arbitrary strain-hardening materials. Comparing this J in an arbitrary problem with the experimentally determined J_c (which then becomes a material property) governing the onset of crack growth, the situation thus can be assessed whether the crack in the given case is on the verge of growing or not.

The relative path independence (within $\pm 3\%$ variation) of the computed J integral indicates that it is, indeed, a valid parameter to be used in a ductile fracture initiation criterion. As stated earlier, the criterion of critical J_c is only a criterion for initiation of crack growth without any statement of stability or instability of such a crack growth. Typically, cracks do not begin to propagate abruptly in elastic-plastic solids. Instead it is usual that the initiation of crack extension is followed by stable growth under continuous increase of the applied load or at least of the loadpoint displacement. Ultimately, the required increase for continuing quasistatic crack advance falls to zero, and unstable propagation follows. Sometimes the stable growth phase is so unnoticeable that initiation and propagation are essentially coincident. This is often the case for "plane strain fracture" under small-scale yield conditions. However, the extents of stable crack growth in "plane stress" situations, in the sheets, can be substantial, as observed by Broek,[16] Link and Muntz,[17] and Bergkvist and Andersson.[18] Thus it is felt that a realistic analytical framework of fracture must include not only models for initiation of crack growth but also models for subsequent stable crack growth, and especially for its terminal loss of stability. Such a finite-element modeling of stable crack growth, involving the translation of entire "singular" near-tip elements, currently is being carried out, and the results will be reported in a subsequent paper.

Appendix: Incremental Elastic-Plastic Constitutive Law

Using the J_2 theory of Huber-Mises-Hencky, the yield criterion is written as

$$f(J_2) = 3/2\sigma'_{ij}\sigma'_{ij} - \sigma_y^2 = 0$$

where

$$\sigma'_{ij} = \sigma_{ij} - \tfrac{1}{3}\sigma_{KK}\delta_{ij} \qquad \text{(A1)}$$

The flow rule $d\epsilon_{ij}^{P} = d\lambda\ (\partial f/\partial\sigma_{ij})$ is used. The Prager-Ziegler hardening rule, with the subsequent yield surface representation,

$$f(\sigma_{ij}-\alpha_{ij}) = 0; \qquad d\alpha_{ij} = d\mu(\sigma_{ij}-\alpha_{ij}) \tag{A2}$$

is used. For infinitesimal increments, it is seen that

$$d\mu = \left[\left(\frac{\partial f}{\partial\sigma_{mm}}\right) d\sigma_{mn}\right] \Big/ \left[(\sigma_{K\ell}-\alpha_{K\ell})\frac{\partial f}{\partial\sigma_{K\ell}}\right] \tag{A3}$$

Using Eqs. (A1-A3), the classical theory of plasticity yields, after some manipulations, the following relation between incremental stresses and incremental total strains:

$$d\sigma_{ij} = E^{t}_{ijk\ell} d\epsilon^{t}_{k\ell} \tag{A4}$$

where $E^{t}_{ijk\ell}$ is represented in matrix form for plane strain and plane stress cases, respectively, below.

1. Plane Strain Case

$$d\sigma_x = \left\{\frac{(1-\nu)E}{(1+\nu)(1-2\nu)} - \frac{S_1^2}{S}\right\} d\epsilon^{t}_{x} + \left\{\frac{\nu E}{(1+\nu)(1-2\nu)} - \frac{S_1S_2}{S}\right\} d\epsilon^{t}_{y} - \frac{S_1S_3}{S} d\gamma^{t}_{xy}$$

$$d\sigma_y = \left\{\frac{\nu E}{(1+\nu)(1-2\nu)} - \frac{S_1S_2}{S}\right\} d\epsilon^{t}_{x} + \left\{\frac{(1-\nu)E}{(1+\nu)(1-2\nu)} - \frac{S_2^2}{S}\right\} d\epsilon^{t}_{y} - \frac{S_2S_3}{S} d\gamma^{t}_{xy}$$

$$d\tau_{xy} = -\frac{S_1S_3}{S} d\epsilon^{t}_{x} - \frac{S_2S_3}{S} d\epsilon^{t}_{y} + \left\{\frac{E}{2(1+\nu)} - \frac{S_3^2}{S}\right\} d\gamma^{t}_{xy}$$

where

$$S_1 = \frac{E}{(1+\nu)(1-2\nu)}\left\{(1-\nu)\frac{\partial f}{\partial\sigma_x} + \frac{\nu\partial f}{\partial\sigma_y}\right\}$$

$$S_2 = \frac{E}{(1+\nu)(1-2\nu)}\left\{\frac{\nu\partial f}{\partial x} + (1-\nu)\frac{\partial f}{\partial\sigma_y}\right\}$$

$$S_3 = \frac{E}{(1+\nu)}\frac{\partial f}{\partial\tau_{xy}}$$

$$S = CQ + S_1\frac{\partial f}{\partial\sigma_x} + S_2\frac{\partial f}{\partial\sigma_y} + 2S_3\frac{\partial f}{\partial\tau_{xy}}$$

$$\frac{\partial f}{\partial\sigma_x} = \frac{3}{2}\left[(\sigma_x-\alpha_x) - (\sigma_y-\alpha_y)\right]$$

$$\frac{\partial f}{\partial\sigma_y} = \frac{3}{2}\left[(\sigma_y-\alpha_y) - (\sigma_x-\alpha_x)\right]$$

$$\frac{\partial f}{\partial\tau_{xy}} = 3(\tau_{xy}-\alpha_{xy}); \quad Q = \left(\frac{\partial f}{\partial\sigma_x}\right)^2 + \left(\frac{\partial f}{\partial\sigma_y}\right)^2 + 2\left(\frac{\partial f}{\partial\tau_{xy}}\right)^2$$

The parameter C in the foregoing corresponds to the slope of the uniaxial stress-strain curve, and the parameters α_x, α_y, and α_{xy} are obtained from (A2) and (A3).

2. Plane Stress Case

$$d\sigma_x = [E^* - S_1^2/S]d\epsilon^{t}_{x} + [\nu E^* - (S_1S_2)/S]d\epsilon^{t}_{y} - [(S_1S_3)/S]d\gamma^{t}_{xy}$$

$$d\sigma_y = [\nu E^* - (S_1S_3)/S]d\epsilon^{t}_{x} + [E^* - S_2^2/S]d\epsilon^{t}_{y} - [(S_2S_3)/S]d\gamma^{t}_{xy}$$

$$d\tau_{xy} = -[(S_1S_3)/S]d\epsilon^{t}_{x} - \nu(S_2S_3)/S]d\epsilon^{t}_{y} + [E^*(1-\nu)/2 - S_3^2/S]d\gamma^{t}_{xy}$$

where

$$E^* = E/(1-\nu^2); \quad S_1 = E^*[\partial f/\partial\sigma_x + \nu\partial f/\partial_y]$$

$$S_2 = E^*[\nu\partial f/\partial\sigma_x + \partial f/\partial\sigma_y]$$

$$S_3 = E^*(1-\nu)(\partial f/\partial\tau_{xy})$$

The functions S, $\partial f/\partial\sigma_x$, $\partial f/\partial\sigma_y$, $\partial f/\partial\tau_{xy}$ and Q are derived in a similar way as in the plane strain case.

Acknowledgments

This work was initiated under the support of the U.S. Air Force Office of Scientific Research under Grant 74-2667. In recent months, the authors' work in the basic finite-element methods used here has been supported by the National Science Foundation under Grant ENG 74-21346. The authors gratefully acknowledge these supports.

References

[1] Hutchinson, J. W., "Singular Behavior at the End of a Tensile Crack in a Hardening Material," *Journal of Mechanics and Physics of Solids*, Vol. 16, Jan. 1968, pp. 13-31.

[2] Rice, J. R. and Rosengren, G. F., "Plane Strain Deformation Near a Crack Tip in a Power Law Hardening Material," *Journal of Mechanics and Physics of Solids*, Vol. 16, Jan. 1968, pp. 1-12.

[3] Rice, J. R., "A Path Independent Integral and the Approximate Analysis of Strain Concentration by Notches and Cracks," *Journal of Applied Mechanics*, Vol 35, June 1968, pp. 379-386.

[4] Eshelby, J. D., "The Continuum Theory of Lattice Defects," *Solid State Physics*, Vol. III, Academic Press, New York, 1956.

[5] Begley, J. A. and Landes, J. D., "The *J*-integral as a Fracture Criterion," *Fracture Toughness*, American Society for Testing and Materials, ASTM STP 514, 1972, pp. 1-20.

[6] Rice, J. R., Paris, P. C., and Merkle, J. G., "Some Further Results of *J*-Integral Analysis and Estimates," *Progress in Flaw Growth and Fracture Toughness Testing and Materials*, ASTM, STP 536, 1973, pp. 231-245.

[7] Bucci, R. J., Paris, P. C., Landes, J. D., and Rice, J. R., "*J*-Integral Estimation Procedures," *Fracture Toughness*, American Society for Testing and Materials, ASTM STP 514, 1972, pp. 40-70.

[8] Goldman, N. L. and Hutchinson, J. W., "Fully Plastic Crack Problems: The Center-Cracked Strip Under Plane Strain," *International Journal of Solids and Structures*, Vol. II, May 1975, pp. 575-593.

[9] Shih, G. F., "Small-Scale Yielding Analysis of Mixed Mode Plane Strain Crack Problems," Harvard Univ., Rept. DEAPS-1, 1973.

[10] Atluri, S. N., Kobayashi, A. S., and Nakagaki, M., "An Assumed Displacement Hybrid Finite Element Model for Linear Fracture Mechanics," *International Journal of Fracture*, Vol. 11, No. 2, April 1975, pp. 257-271.

[11] Atluri, S. N., Kobayashi, A. S., and Nakagaki, M., "Fracture Mechanics Application of an Assumed Displacement Hybrid Finite Element Procedure," *AIAA Journal*, Vol. 13, No. 36, June 1975, pp. 734-740.

[12] Zienckiewicz, O. C., Valliappan, S., and King, I. P., "Elastic-Plastic Solutions of Engineering Problems, 'Initial Stress' Finite Element Approach," *International Journal for Numerical Methods in Engineering*, Vol. 1, Jan. 1969, pp. 75-100.

[13] Hofmeister, L. D., Greenbaum, G. A., and Evensen, D. A., "Large Strain, Elasto-Plastic Finite Element Analysis," *AIAA Journal*, Vol. 9, July 1971, pp. 1248-1254.

[14] Merkle, J. G. and Corten, H. T., "A *J*-Integral Analysis for the Compact Specimen, Considering Axial Force as Well as Bending Effects," *Journal of Pressure Vessel Technology*, Vol. 96, Nov. 1974, pp. 286-292.

[15] Atluri, S. N., Nakagaki, M., and Chen, W. H., "Fracture Analysis Under Large-Scale Plastic Yielding: A Finite Deformation, Embedded Singularity, Elasto-Plastic Incremental Finite Element Solution," *10th National Symposium on Fracture*, Philadelphia, Pa., Aug. 1976; also American Society for Testing and Materials (to be published).

[16] Broek, D., "Some Considerations on Slow Crack Growth," *International Journal of Fracture Mechanics*, Vol. 4, 1968, pp. 19-34.

[17] Link, F. and Muntz, D., "Fracture Toughness Investigations of a Titanium Alloy," *Material Prüf*, Vol. 13, Dec. 1971, p. 407.

[18] Bergkvist, and Andersson, H., "Plastic Deformation at a Stably Growing Crack-tip," *International Journal of Fracture Mechanics*, Vol. 8, No. 2, June 1972, pp. 139, 156.

[19] Tada, H., Paris, P. C., and Irwin, G. R., "The Stress Analysis of Cracks Handbook," Del Research Corp., Hellertown, Pa., 1973.